Modular microscopy (ModMicro) solution for volumetric epifluorescence microscopic imaging

Robert Archibald
University of Glasgow
Harriet Bishop
University of Glasgow
Graham Gibson
University of Glasgow
Akhil Kallepalli (Akhil.Kallepalli@glasgow.ac.uk)
University of Glasgow

Article

Keywords:

Posted Date: August 30th, 2023

DOI: https://doi.org/10.21203/rs.3.rs-3293259/v1

Additional Declarations: No competing interests reported.

Modular microscopy (ModMicro) solution for volumetric epifluorescence microscopic imaging

Robert Archibald[1], **Harriet Bishop**[1], **Graham Gibson**[1], **and Akhil Kallepalli**[1,*]

[1]School of Physics and Astronomy, University of Glasgow, Glasgow G12 8QQ, UK
[*]For all correspondence, please contact Dr Akhil Kallepalli., E-mail: Akhil.Kallepalli@glasgow.ac.uk

ABSTRACT

Fluorescence microscopy is a well-known technique for studying biological samples. However, on a global scale, microscopy techniques (beyond brightfield imaging) are inaccessible in some countries. Additionally, proprietary microscopy hardware is not modular and cannot be adapted for different architectures. In this research, we demonstrate a modular epifluorescence microscopy system and image analysis technique developed with the motivation of achieving high-resolution imaging using low-cost modular hardware. We compare the performance of the (1000 GBP) OpenFlexure-inspired epifluorescence ModMicro system to a proprietary epifluorescence microscope. With the epifluorescence ModMicro system, we imaged 'datacubes' of 0.54 x 0.40 x 0.005 mm (in 100 steps of 50 nm each) size. The image data is enhanced with a novel sharpening algorithm. Combined (light sources, microscope hardware and image sharpness enhancement algorithm), a complete system for epifluorescence microscopy that is globally accessible and cost-effective is presented.

Introduction

Fluorescence microscopic imaging was first developed as a transmission microscopy approach[1]. This technique was further developed into the now widely used epifluorescence imaging setup[2,3]. Subsequent innovations such as dichroic mirrors contributed to enabling a reflection-based approach (that is now standard)[4]. This technique transformed the way the microscopic world is observed, particularly in life sciences where it enabled the visualisation of cells and their internal structures with fluorophores enabling complex labelling and observation of cells.

Fluorophores are biological labels that absorb and emit light due to the Stokes shift (wherein the light absorbed by the fluorophores is emitted at a longer wavelength)[5]. For example, green fluorescent protein (GFP)[6] which when excited by ultraviolet (395 nm) and blue light (488 nm) has an emission peak wavelength of 509 nm (green) depending on the specific type of GFP[7,8]. Typically, an epifluorescence microscope will have emission, excitation and dichroic filters to reduce noise and limit excess light, increasing the fluorophore's effectiveness. However, the variability of the hardware in quality and capability is substantial, and so are the output images produced by the microscopes. For instance, epifluorescence microscopes have shown the ability of volumetric imaging from 3D reconstructions[9], are widely used for live cell imaging[10], virus detection and counts in natural waters[11], and are essential in studies with zebrafish[12,13].

The main limitations of epifluorescence microscopes are their spatial resolution, which is in turn limited by the numerical aperture of the objective, the wavelength of the incident light on the sample and the limited depth of field. As a result, only thin samples can be effectively imaged. These limitations have led to the development of more advanced microscopy techniques such as confocal microscopy and stimulated emission depletion (STED) microscopy (which is a form of superresolution microscopy that beats the diffraction limit)[4,5]. While all these techniques have their advantages and disadvantages across many conditions for a microscopist, fluorescence microscopy fundamentally continues to be explored.

This research is a step towards making this technique accessible through open-access hardware and low-cost designs. Our approach to the development of a modular epifluorescence microscope uses the OpenFlexure microscope[14,15] as a starting point. Other open-sourced 3D-printed microscopes such as UC2, which has accomplished 2D super-resolution imaging using structured illumination microscopy (SIM)[16,17], the miCube open microscope[18] and FlyPi[19] offer alternative approaches. However, our choice is based on the overall stage stability and modular components that allow us to deconstruct the OpenFlexure microscope, and include our designs for achieving a ModMicro system. Subsequently, we engineered novel and redesigned components, along with integrated light sources (ModLight[20]), to build an epifluorescence microscope for under 1000 GBP. The novel sharpening algorithm applied to the images enhances the images to improve their quality.

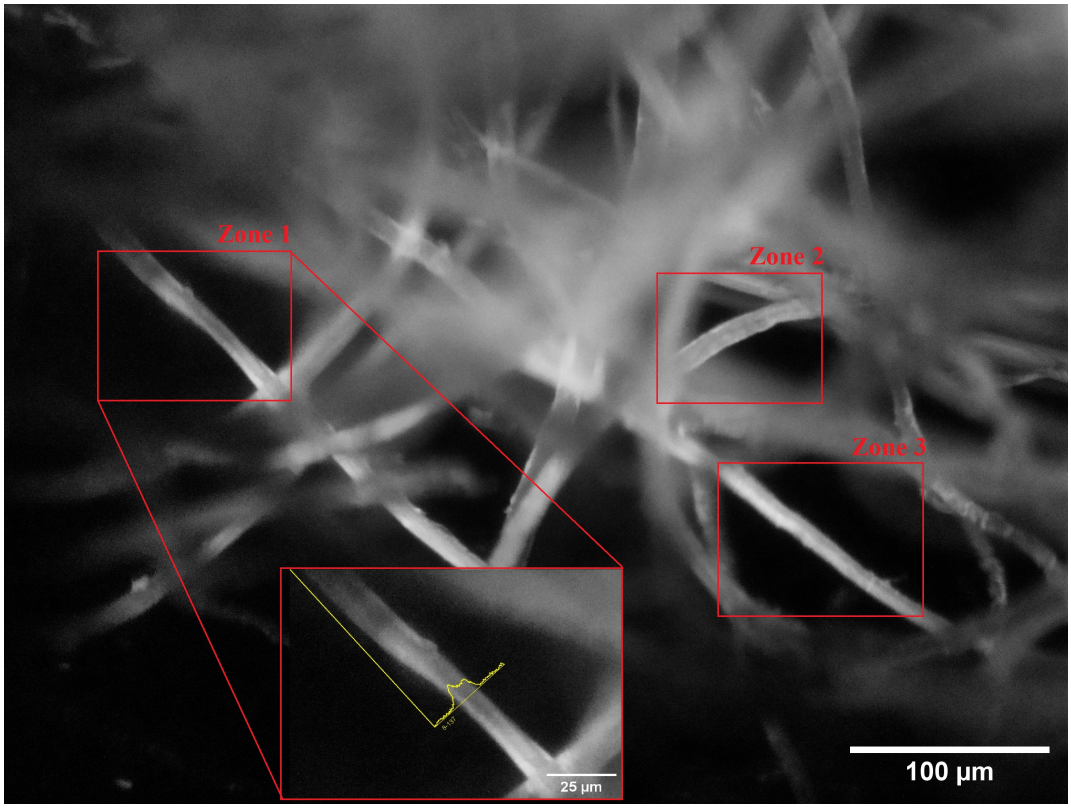

Figure 1. Tissue paper dyed in fluorescein imaged with the ModMicro epi-fluorescence microscope and a 10x, 0.25 NA infinity corrected objective. The red boxes indicate the three ROI across the sample, showing a line intensity profile for Zone 1, detailed in figure 2. All three ROI, across all three datasets (ModMicro, ModMicro with an intrinsic sharpness enhancement algorithm and a Nikon Ti-Eclipse microscope), are analysed.

Results and Discussion

The images in this study are acquired from two microscope systems. These include our contribution, the ModMicro epifluorescence microscope, and the Nikon Ti-Eclipse microscope. The z-stack images were acquired and compared, both qualitatively and quantitatively. The z-stack datasets of the sample are assessed for sharpness[21] in three regions of interest (ROI), as shown in Figure 1. The comparison showed that the images collected by the ModMicro microscope are comparable to the standard microscope images and further improved using the proposed intrinsic sharpness enhancement algorithm (as detailed in Table 1).

Table 1. The sharpness values of features in the three indicated zones using image data from the ModMicro epifluorescence microscope, sharpness-enhanced epifluorescence images and Nikon Ti-Eclipse microscope. *Left* indicate the first half of the line intensity profile and *Right* the second half, respectively. As shown in units of physical size (μm, calculated from pixel size and number of pixels), the key inference drawn is that the intrinsic sharpness enhancement algorithm consistently improves the sharpness of the ModMicro images, resulting in sharpness results comparable to the Nikon Ti-Eclipse microscope.

Imaging System	**Zone 1**	**Zone 2**	**Zone 3**
	Left (μm)	Left (μm)	Left (μm)
ModMicro	26.50	12.58	12.09
ModMicro Data with Sharpness Algorithm	23.25	12.25	11.27
Nikon Ti-Eclipse	26.77	11.94	13.50

The data from all three zones are assessed for sharpness using line profiles of pixel values (data from all profiles, images and imaging systems are detailed in **Supplementary 1**). Zone 1's intensity profiles (Figure 2) of the sample show clear comparable sharpness of the features with a marginal enhancement using the sharpness enhancement algorithm (ModMicro Sharpened, in the graph). In the pixel value profiles, the shoulders are much steeper for the ModMicro system data when compared to the Nikon data. This is interpreted as a better contrast of pixel values in resolving the features using our proposed system and

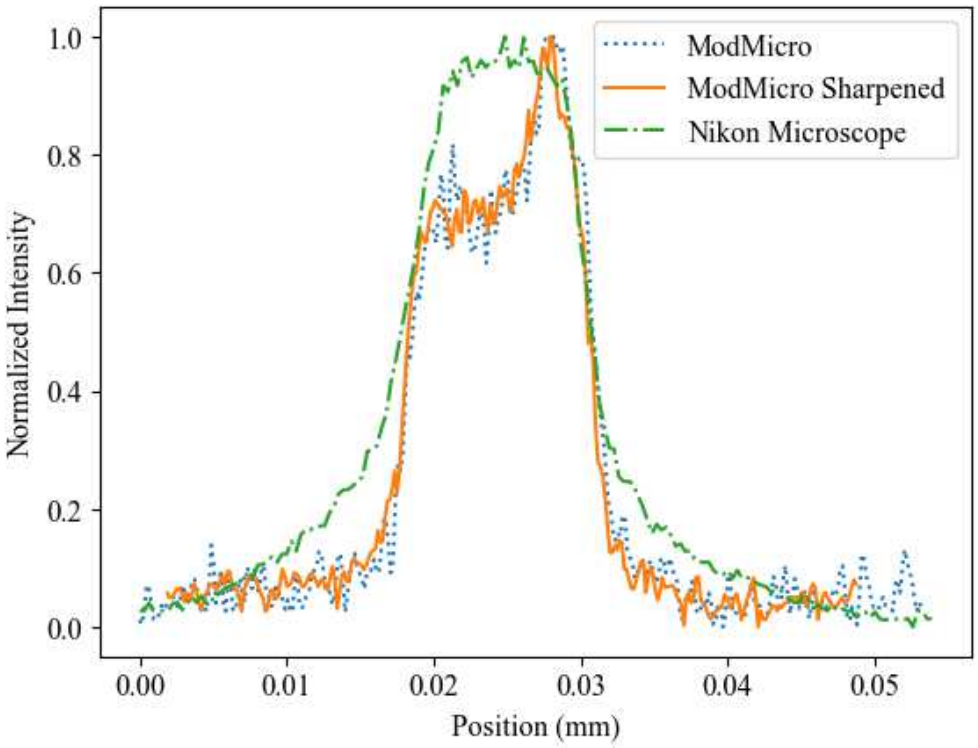

Figure 2. Determination of the sharpness profile of ModMicro, ModMicro with an intrinsic sharpness enhancement algorithm and a Nikon Ti-Eclipse microscope. Plotting normalised intensity against the lateral position in x-y directions determines the FWHM of the axial sharpness summarised in Table 1.

sharpness enhancement algorithms. Additional inferences from the profiles show variations in pixel values (Zone 1, Figure 1) indicative of features that could not be resolved in the Nikon microscope. For instance, in Zone 1, the object includes a 'dark' spot in the middle of the individual feature. This, in terms of changes in pixel values, could not be detected on the Nikon Ti-Eclipse microscope data. The sharpness of the resolved features is further assessed for each ROI (Zone 2 data illustrated in figure 3) and their respective fitted sigmoidal functions.

Methods

The methods in this research include hardware and image processing algorithm contributions. The hardware is a complete solution for epifluorescence imaging while the data from this microscope system is the input for the sharpness enhancement algorithm. Finally, the data from the ModMicro epifluorescence system and the sharpness-enhanced algorithm are compared to data from a standard Nikon Ti-Eclipse microscope. The ModMicro epifluorescence microscope is initially operated in transmission mode to determine the field of view and resolution using a micron ruler (0.01mm Stage Micrometer Microscope Camera Calibration Slide, MUHWA; calibration procedure in **Supplementary 1**). A lens-cleaning tissue (MC-5, Thorlabs, Inc.) dipped in a fluorescein solution, between a cover slip (0.17 mm thick) and a glass slide, was used for imaging.

The ModMicro epifluorescence microscope data is compared to collected data from a Nikon Ti-Eclipse microscope equipped with a Zyla 5.5 sCMOS detector (21.8 mm sensor size (diagonal) with 6.5 μm pixel size and 2560 x 2160 active pixels) and a 20x, 0.5 NA infinity-corrected objective (with a 200 mm tube lens in the optical path). This Nikon Ti-Eclipse inverted microscope is capable of epifluorescence microscopy, amongst other capabilities. The light source used is a mercury lamp equipped with a 500 nm short-pass filter. The optical path includes a 460-490 nm excitation filter, a 496-547 nm dichroic mirror and a 495-545 nm emission filter. We identify and evaluate the same region of the sample to establish a direct comparison in the sharpness of the microscopes.

Modular epifluorescence microscope

The OpenFlexure microscope main body (OFMMB) is a central component of the ModMicro system. The choice is made based on the accessibility of the platform and the flexibility to make necessary changes in this study. Being the most up-to-date version

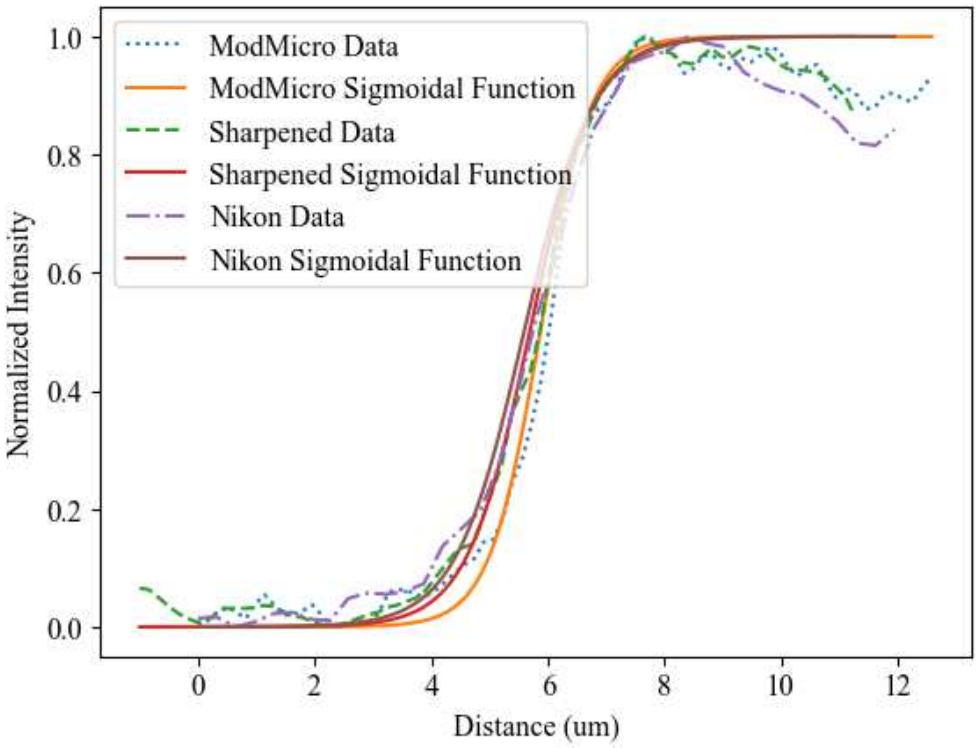

Figure 3. Analysis of the sharpness profile of ModMicro, ModMicro with an intrinsic sharpness enhancement algorithm (labelled 'Sharpened') and a Nikon Ti-Eclipse microscope (labelled 'Nikon'). Plotting normalised intensity against axial position in x-y directions with a sigmoidal function fitted over the data to determine the sharpness of each microscope, by calculating the distance between the highest to the lowest values of the respective sigmoidal functions.

of the OpenFlexure apparatus, this is the most appropriate model to use but the optical components of the epifluorescence microscope are interchangeable with the OpenFlexure Delta stage microscope with a customised base. The OFMMB has three flexible actuators with a 12 x 12 x 4 mm adjustable stage range and uses stepper motors for tens of nanometer stage and objective control in x, y and z directions. The imaging is done using a Raspberry Pi camera V2 (Sony IMX219 CMOS sensor with 8 megapixels in a 3280 x 2464 format). The stepper motors (Part number: 28BYJ-48) are controlled by a motor control board that connects to the same Raspberry Pi used to operate the microscope and the camera. For illumination, we integrated the ModLight devices[20] which includes a narrow spectral bandwidth blue LED (central wavelength of 480 nm). The use of a narrow bandwidth LED makes the excitation filter redundant, simplifying our system.

The optics module was designed in the freely available design software OpenSCAD. Figure 5 shows the overview of the novel 3D-printed optics module. The two primary cubes are each one piece of 50 x 50 x 50 mm dimensions and custom-designed for specific attachments. **Cube1** has two self-tap M3 screw holes which enable the Raspberry Pi camera module to be held in place at the optimal alignment of the system. The Raspberry Pi attachment also has two M6 through holes for attachment to an optical bench. Within **Cube1** there is a slot set at 45 degrees that allows for a 25 x 35 mm silver-coated mirror placed into a 3D-printed mirror holder to be inserted. At the top and the bottom of **Cube1** are circular cut-outs where magnets are glued to magnetically attach and align with **Cube2** and an optical bench.

Cube2 also has circular cut-outs where magnets are glued to magnetically attach and align with Cube1 and a 3D-printed tube lens holder. This cube has two slots; the slot set at 0 degrees allows for a 3D-printed holder tray to be passed through the cube, allowing the user to choose from a selection of different emission filters. A second slot at 45 degrees and a similar holder tray allow different dichroic mirrors to be selected.

Attached to the OFMMB is a standard RMS threaded 3D printed objective holder. The attachment on the objective holder is the same as the OFM objective mount. We used a 10x, 0.25 NA and a 4x, 0.1 NA infinity-corrected objective lens. Due to the design of the optics module, a 125mm focal length achromatic doublet lens to correct for the tube length of the infinity corrected Olympus objectives was used. This meant the true magnification and relative field of view were different from that stated in the objectives.

From equation 1 we find the desired magnification of the system to optimise the effective field number, the eye-piece

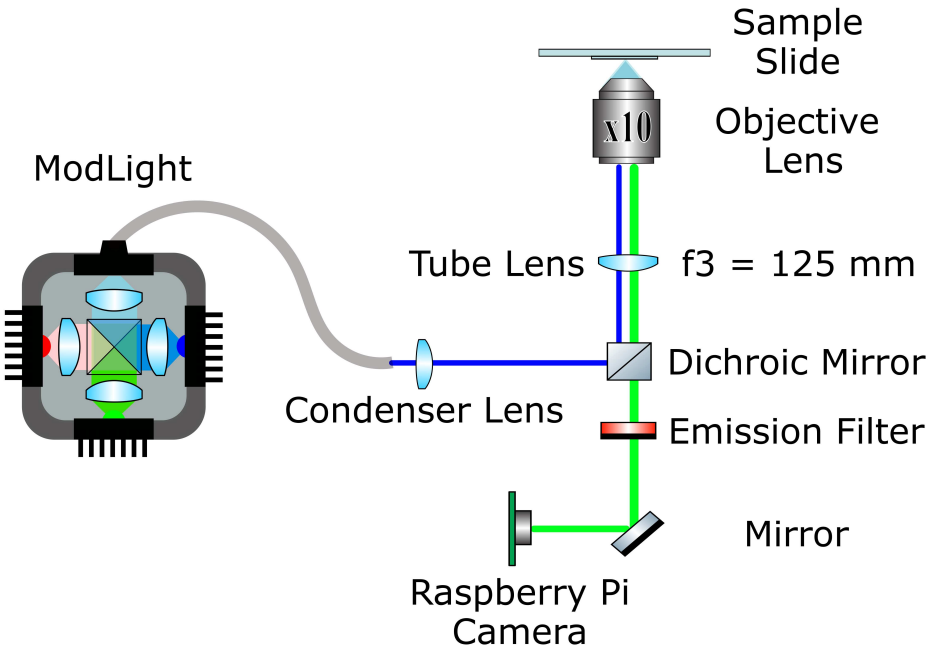

Figure 4. The ModMicro epifluorescence microscope system combines a novel microscope design with modular light sources (ModLight[20]). The setup includes a condenser lens (f = 5 mm), dichroic mirror (25 x 36 mm longpass dichroic mirror, 505nm cut-on), tube lens (f = 125 mm), objective lens (RMS10X - 10X Olympus Plan Achromatic Objective, 0.25NA) and emission filter (CWL=535nm, BW +22nm). The imaging is achieved using a Raspberry Pi camera. Note that our choice of narrow-band wavelength-specific LEDs has excluded the need for an excitation filter.

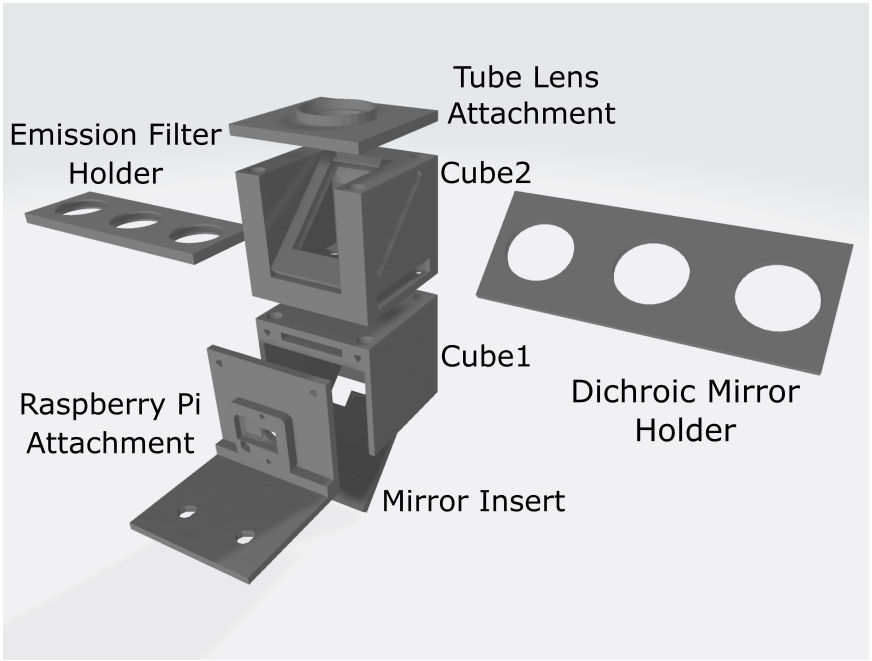

Figure 5. Novel 3D printed optical components of the epifluorescence microscope.

aperture at the image plane, i.e., the field of view, as M = 0.21, assuming a field number of 22. The limitations of the hardware design mean the minimum distance between the sensor and the tube lens is 110mm, so the minimum focal length of the tube lens can be 110 mm. We use a 125 mm focal length achromatic doublet lens. Therefore, our true Magnification from equation 2

is M = 2.8 for 4x, 0.1 NA infinity-corrected objective lens with an effective field number of 1.08 mm. The true magnification for the 10x, 0.25 NA infinity-corrected objective lens is M = 6.95 with an effective field number of 0.66 mm.

Intrinsic sharpness enhancement

All applications of microscopy rely on the separation of features in an image, i.e. resolving objects, and therefore, image enhancement is an essential step in the workflow. Used along with the novel microscope hardware but applicable independently, we developed sharpness enhancement methods to eliminate the inherent blurring that occurs from z-stack data acquisition. The out-of-focus light captured by the imaging sensor increases as the sample moves away from the focal point of the microscope objective. An enhancement algorithm is developed that achieves sharpening by removing low spatial frequency regions in the image. This is done by subtracting the low pass filtered (LPF) version of that image from itself. Such a filter is constructed using an $n \times n$ matrix filled with values of $1/n$, for which there exists an optimised size (or n value). Therefore, an additional step in the workflow is required to find this value. For this, three sharpness metrics are used.

Sharpness Metrics

Three sharpness metrics were proposed for this purpose, each utilising the pixel values of the image to measure the gradient across image features, and thus its inherent sharpness. Every image can be deconstructed spatially into local neighbourhoods, providing context to individual pixels. The differentiating factor between each metric is the choice of the size of these neighbourhoods, and the choice itself is key to its effectiveness for a given data set. Deciding the best metric was supervised, wherein the performance of the metrics was analysed visually. An onion epidermis z-stack was used as test data to select the best metric for the final version of the sharpening algorithm.

The first metric applies a Laplacian operator, L_{xy} to each image via a convolution. This type of filter is commonplace in edge detection applications to detect discontinuities at any orientation. Once applied to the image, the pixel values are squared and averaged to produce a 'sharpness score'[22]. The higher the score, the sharper the image.

$$L_{xy} = \begin{bmatrix} 0 & 1 & 0 \\ 1 & -4 & 1 \\ 0 & 1 & 0 \end{bmatrix}$$

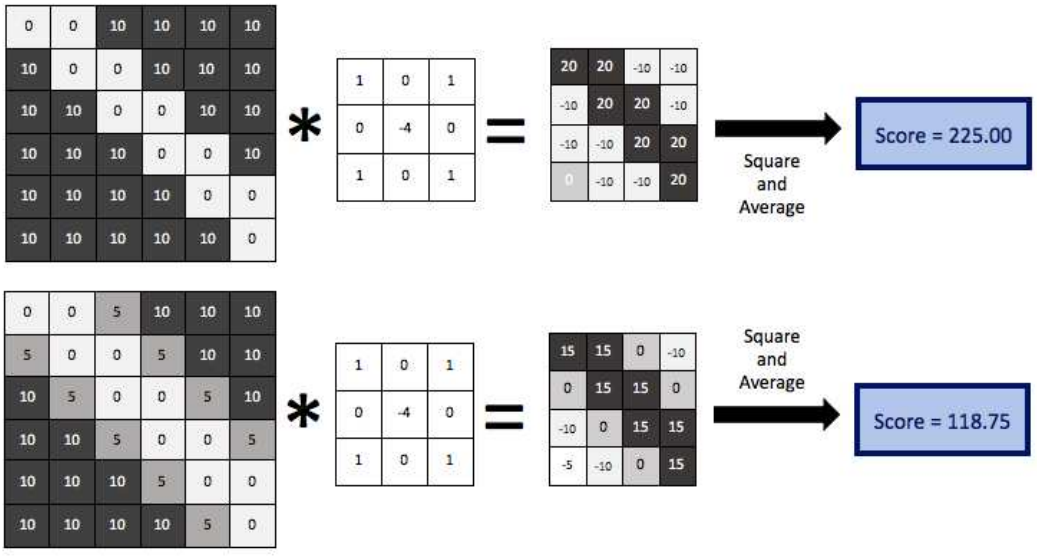

Figure 6. Demonstration of how the Laplacian operator can be used to distinguish between images of different sharpness. A convolution between the image and this operator produces a compressed matrix retaining key image features. This resultant matrix can be squared and averaged to produce a 'sharpness score', from which the sharpest image can be determined.

The second metric evaluates a specific neighbourhood as opposed to the image as a whole. A line of pixels specified by the user is used to obtain intensity as a function of position. This yields peaks which correspond to the features in the image. The full-width half maximum (FWHM) of the largest peak is obtained using a built-in peak finding package in Python, and these values are used directly as a measure of sharpness. Here, a narrow FWHM is indicative of an in-focus, sharp image. The same

package can be used to identify the number of peaks in this plot, from which a third metric arises. Here, a greater number of peaks indicates a larger number of distinguishable features and thus a sharper image.

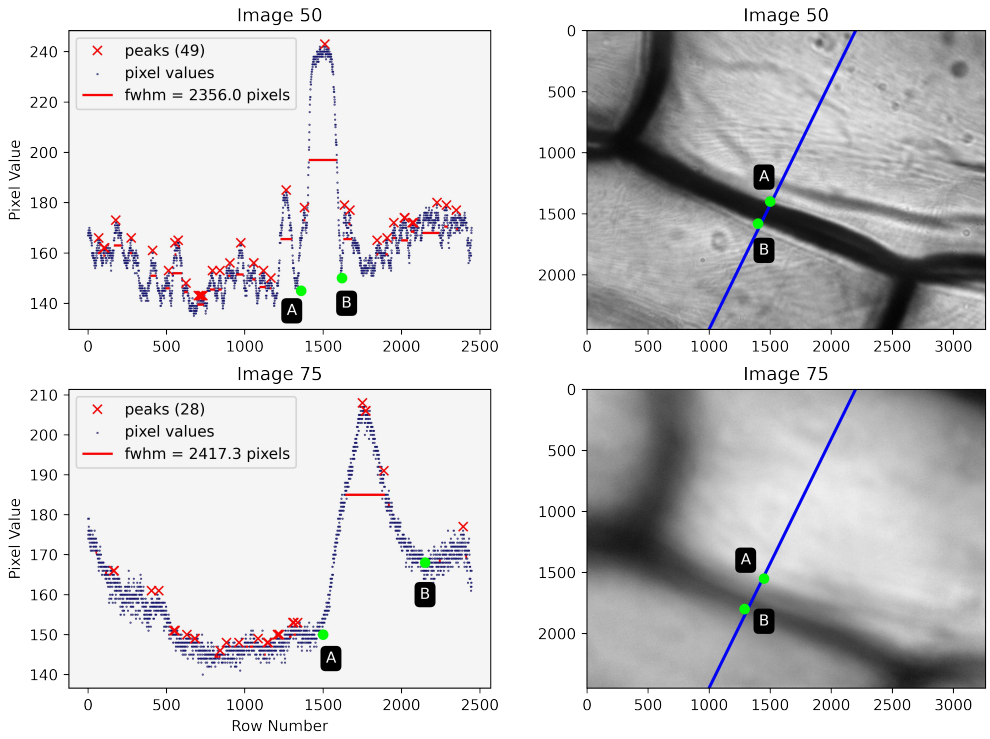

Figure 7. An alternative approach for determining image sharpness (SM2 and SM3). A line is plotted perpendicular to the cell wall in an image of an onion epidermis and the intensity of the pixel at each point on the line is plotted as a function of the row number. Points A and B mark the position of the cell wall and subsequently the turning points of the resultant peak. The FWHM and number of peaks are measured as their value is used to compare image sharpness.

Conclusions

The primary objective we set out to achieve was to make a cost-effective and modular solution to advanced microscopy techniques, beginning with an epifluorescence microscopy system. The use of narrow-bandwidth LED sources, individually selected for the particular sample being investigated, allows for a simpler, and more cost-effective, optical setup that does not require the use of narrow-band excitation filters. The 3D-printed hardware and image sharpness enhancement algorithms combined are a complete solution for imaging samples. The imaging capability of the ModMicro epifluorescence system can be quantitatively compared to the proprietary microscope (within the scope of this study). Subsequent work will focus on strengthening the epifluorescence microscope system with future versions, and continue to develop additional techniques to extend the constellation of modular microscopy hardware (https://github.com/AkhilKallepalli/ModMicroUofG).

References

1. Zanacchi, F. C., Bianchini, P. & Vicidomini, G. Fluorescence microscopy in the spotlight (2014).
2. Ellinger, P. Fluorescence microscopy in biology. *Biol. Rev.* **15**, 323–347 (1940).
3. Ellinger, P. Lyochromes in the kidney. with a note on the quantitative estimation of lyochromes. *Biochem. J.* **32**, 376 (1938).
4. Wollman, A. J., Nudd, R., Hedlund, E. G. & Leake, M. C. From animaculum to single molecules: 300 years of the light microscope. *Open biology* **5**, 150019 (2015).
5. Webb, D. J. & Brown, C. M. Epi-fluorescence microscopy. In *Cell imaging techniques*, 29–59 (Springer, 2012).
6. Shimomura, O., Johnson, F. H. & Saiga, Y. Extraction, purification and properties of aequorin, a bioluminescent protein from the luminous hydromedusan, aequorea. *J. cellular comparative physiology* **59**, 223–239 (1962).
7. Reid, B. G. & Flynn, G. C. Chromophore formation in green fluorescent protein. *Biochemistry* **36**, 6786–6791 (1997).
8. Savchuk, O. A., Silvestre, O. F., Adão, R. M. & Nieder, J. B. Gfp fluorescence peak fraction analysis based nanothermometer for the assessment of exothermal mitochondria activity in live cells. *Sci. reports* **9**, 7535 (2019).
9. Olesker, D., Harvey, A. R. & Taylor, J. M. Snapshot volumetric imaging with engineered point-spread functions. *Opt. Express* **30**, 33490–33501 (2022).
10. Rizzuto, R., Carrington, W. & Tuft, R. A. Digital imaging microscopy of living cells. *Trends Cell Biol.* **8**, 288–292 (1998).
11. Hennes, K. P. & Suttle, C. A. Direct counts of viruses in natural waters and laboratory cultures by epifluorescence microscopy. *Limnol. Oceanogr.* **40**, 1050–1055 (1995).
12. Kinth, P., Mahesh, G. & Panwar, Y. Mapping of zebrafish research: a global outlook. *Zebrafish* **10**, 510–517 (2013).
13. Kaveh, A. *et al.* Selective cdk9 inhibition resolves neutrophilic inflammation and enhances cardiac regeneration in larval zebrafish. *Development* **149**, dev199636 (2022).
14. Collins, J. T. *et al.* Robotic microscopy for everyone: the openflexure microscope. *Biomed. Opt. Express* **11**, 2447–2460 (2020).
15. McDermott, S. *et al.* Multi-modal microscopy imaging with the openflexure delta stage. *Opt. Express* **30**, 26377–26395 (2022).
16. Wang, H., Lachmann, R., Marsikova, B., Heintzmann, R. & Diederich, B. Ucsim2: 2d structured illumination microscopy using uc2. *bioRxiv* 2021–01 (2021).
17. Diederich, B. *et al.* A versatile and customizable low-cost 3d-printed open standard for microscopic imaging. *Nat. communications* **11**, 5979 (2020).
18. Strack, R. The micube open microscope. *Nat. Methods* **16**, 958–958 (2019).
19. Maia Chagas, A., Prieto-Godino, L. L., Arrenberg, A. B. & Baden, T. The€ 100 lab: A 3d-printable open-source platform for fluorescence microscopy, optogenetics, and accurate temperature control during behaviour of zebrafish, drosophila, and caenorhabditis elegans. *PLoS biology* **15**, e2002702 (2017).
20. Gibson, G. M., Archibald, R., Main, M. & Kallepalli, A. Modular light sources for microscopy and beyond (modlight). *HardwareX* e00385 (2022).
21. Ferreira, T. & Rasband, W. Imagej user guide. *ImageJ/Fiji* **1**, 155–161 (2012).
22. Knapper, J. *et al.* Fast, high-precision autofocus on a motorised microscope: Automating blood sample imaging on the openflexure microscope. *J. Microsc.* **285**, 29–39, DOI: https://doi.org/10.1111/jmi.13064 (2022). https://onlinelibrary.wiley.com/doi/pdf/10.1111/jmi.13064.

Acknowledgements

We wish to acknowledge the support of the Leverhulme Trust Early Career Fellowship, EPSRC Impact Acceleration Account (IAA) awards [EP/X5257161/1, EP/R511705/1], EPSRC funding to QuantIC [EP/M01326X/1], University of Glasgow Knowledge Exchange Fund (GKEF), Institute of Physics (IOP), IEEE Photonics Society Seed Grant and the Royal Society. We would like to also thank the incredible assistance and support from Dr Jonathan Taylor, Daniel Olesker and Conall Thompson (Imaging Concepts Group, School of Physics and Astronomy, University of Glasgow) with sample preparation and access to the Nikon Ti-Eclipse microscope.

Author contributions statement

The research idea was led and conceptualised with AK, with key contributions from RA. HB led the development of the sharpness algorithm, its testing and sharing of the datasets for applying this technique. GG and RA assisted in the design and building of the low-cost microscope build and development. The initial draft was prepared by AK, with all authors contributing to the manuscript.

Supplementary Files

This is a list of supplementary files associated with this preprint. Click to download.

- ModMicroEpiSupplementaryFile.pdf